

# Fractal Structure of Hastings–Levitov Patterns Restricted in a Sector Geometry

F. Mohammadi<sup>1</sup>, A. A. Saberi<sup>2,\*</sup> and S. Rouhani<sup>1</sup>

<sup>1</sup> *Department of Physics, Sharif University of Technology, P.O. Box 11155-9161, Tehran, Iran.*

<sup>2</sup> *School of Physics, Institute for Research in Fundamental Sciences (IPM), P.O.Box 19395-5531, Tehran, Iran.*

(Dated: November 8, 2018)

A generalized form of the Hastings and Levitov (HL) algorithm for simulation of diffusion-limited aggregation (DLA) restricted in a sector geometry is studied. It is found that this generalization with uniform measure produces "wedge-like" fractal patterns in the physical space, whose fractal dimension and anisotropy exponent depend significantly on the opening angle  $\beta$  of the sector. The morphological properties and the overall shape of the patterns are analyzed by computing the angular two-point density correlation function of the patterns. We also find that the fractal dimension of the patterns with sinusoidal distributed measure depend weakly on  $\beta$  with almost the same dimension as the radial DLA cluster. The anisotropy exponent and the visual appearance of the patterns in this case are shown to be compatible with those of the advection-diffusion-limited aggregation (ADLA) clusters.

PACS numbers: 61.43.Hv, 82.40.Ck, 68.43.Jk, 64.60.al

## I. INTRODUCTION

Diffusion-limited aggregation (DLA) was originally introduced by Witten and Sander [1] in 1981 to model the aggregates of metal particles formed by adhesive contact in low concentration limit. This model has been then shown to describe many pattern forming processes including dielectric breakdown [2], electrochemical deposition [3, 4], viscous fingering and Laplacian growth [5]. One of the standard approaches to simulate a Laplacian field is by random walkers, which are launched from the periphery of the system and diffuse toward the growing cluster and freeze on it. This procedure is equivalent to solving Laplace equation outside the aggregated cluster with an appropriate boundary conditions. The walker sticks to a point on the surface of the aggregate with a probability proportional to the harmonic measure there [6].

Another powerful method for studying such growth processes in two-dimensions, is the iterated stochastic conformal mapping [7–9], which is known as Hastings and Levitov (HL) method.

Since DLA enhances the instability of growth, the resulting cluster is highly ramified and branched. The procedure of the proliferation of the fingers in the fractal structure of DLA is one of its complexity sources which is one of the purposes of the present paper to deal with.

The HL method is based on the fact that there exists a conformal map that maps the exterior of the unit circle in the mathematical  $w$ -plane to exterior of the cluster of  $n$  particles in the physical  $z$ -plane. The complicated harmonic measure in the physical space then changes to a simple measure: a uniform distribution in the mathematical space. The HL algorithm can be also used for more generalized growth models for which the probabil-

ity measure is not uniform in the mathematical plane. In a part of this paper, we also study the statistical and morphological properties of the fractal patterns produced by a novel generalization of the HL algorithm with both uniform and non-uniform probability measures in the  $w$ -plane. We restrict the algorithm to attribute the measure in the  $w$ -plane to a sector of opening angle  $\beta$ . We find that this restriction which breaks the radial symmetry in the growth process, yields fractal patterns whose dimensions depend on whether uniform or non-uniform distribution is used for the measure. For the uniform distribution, the patterns looks like those of DLA in a wedge but with fractal dimension depending on the opening angle  $\beta$ . However for the non-uniform distribution of the measure, we find that the statistical properties of the patterns is compatible with advection-diffusion-limited aggregation (ADLA) [10] and their fractal dimensions take values close to that of radial DLA i.e.,  $d_f = 1.71$  with a weak dependence on the opening angle  $\beta$ .

Bazant *et al.* [10] proposed a method based on time-dependent conformal maps to model a class of non-Laplacian growth processes such as ADLA in a background potential flow. They showed that in spite of dramatic increases in anisotropy, the fractal dimension of the patterns is not affected by advection and takes the same value as for radial DLA clusters.

The fractal dimension of the patterns is already shown to be affected by the geometrical factors. Stepanov and Levitov [11] obtained dimensions as low as  $d_f = 1.5$  for simulations of anisotropic growth (a different anisotropy that we consider in this paper) using the noise-controlled HL algorithm. A similar result reported in [12] for DLA with anisotropic perturbations. Davidovitch *et al.*, [13] introduced growth models that are produced by deterministic itineraries of iterated conformal maps with different dimensions. In channel geometry, the fractal dimensions  $d_f = 1.67$  [14] and  $d_f = 1.71$  [15] are reported for periodic and reflecting boundary conditions, respectively.

---

\*Electronic address: [a.saberi@ipm.ir](mailto:a.saberi@ipm.ir)

The comparison of the ensemble average of DLA cluster density with the noise-free Saffman-Taylor viscous fingers [5] have been the subject of various studies in both channel and wedge geometries [16–19].

There has been shown in [20] that there exists a critical angle  $\eta \approx 60^\circ - 70^\circ$  in viscous fingers and DLA growing in a wedge, indicative of a typical angular spread of a major finger. In this paper, for the patterns produced by restricted HL algorithm with uniform measure, we find that their visual appearance like a DLA cluster in a wedge and we compute the average angle between two major fingers. To estimate the angle, we measure the angular density-density correlation function. We also obtain the relation between the minimum opening angle of a wedge which contains the cluster in the  $z$ -plane, and the opening angle  $\beta$  considered in the  $w$ -plane.

## II. RESTRICTED HL ALGORITHM IN A SECTOR GEOMETRY

Hastings and Levitov (HL) employed the conformal-mapping tool to describe the complicated boundary of a growing DLA cluster. Their approach [7] was based on iteratively applying the function  $\phi_{\lambda,\theta}(w)$  which maps a unit circle to a circle with a bump of linear size  $\sqrt{\lambda}$  at the point  $w = e^{i\theta}$ ,

$$\phi_{\lambda,0}(w) = w^{1-a} \left\{ \frac{1+\lambda}{2w}(1+w) \left[ 1 + w + w \left( 1 + \frac{1}{w^2} - \frac{2}{w} \frac{1-\lambda}{1+\lambda} \right)^{\frac{1}{2}} \right] - 1 \right\}^a, \quad (1)$$

$$\phi_{\lambda,\theta}(w) = e^{i\theta} \phi_{\lambda,0}(e^{-i\theta}w). \quad (2)$$

The parameter  $0 \leq a \leq 1$  determines the shape of the bump, for higher  $a$  the bump becomes elongated in the normal direction to the boundary  $\partial\mathcal{C}$  (e.g., it is a line segment for  $a = 1$ ). In this paper we set  $a = \frac{1}{2}$  for which the bump has a semi-circle shape.

A cluster  $\mathcal{C}_n$  consisting of  $n$  bumps can be obtained by using the following map on a unit circle

$$\Phi_n(w) = \phi_{\lambda_1,\theta_1} \circ \phi_{\lambda_2,\theta_2} \circ \dots \circ \phi_{\lambda_n,\theta_n}(w), \quad (3)$$

which corresponds to the following recursive relation for a cluster  $\mathcal{C}_{n+1}$ ,

$$\Phi_{n+1}(w) = \Phi_n(\phi_{\lambda_{n+1},\theta_{n+1}}(w)). \quad (4)$$

In order to have bumps of fixed-size on the boundary of the cluster, since the linear dimension at point  $w$  is proportional to  $|\Phi'_n(w)|^{-1}$ , one obtains

$$\lambda_{n+1} = \frac{\lambda_0}{|\Phi'_n(e^{i\theta_{n+1}})|^2}. \quad (5)$$

To produce an isotropic radial DLA, the harmonic measure of the  $n$ -th growth probability  $p(z, n)$  has to be conformally mapped onto a constant measure  $p(\theta_n) = \frac{1}{2\pi}$

on a unit circle i.e.,  $0 \leq \theta_n \leq 2\pi$  (more details of the simulation algorithm which have been also considered in this paper are given in our previous work [21]).

In this paper we use a generalized form of the HL algorithm in which  $\theta_n$ s are restricted to be selected from a fixed interval  $0 \leq \theta_n \leq \beta$  on a unit circle, with both uniform and non-uniform measures. This measure

$$\begin{cases} p(\theta_n) & 0 \leq \theta_n \leq \beta \\ 0 & \text{otherwise,} \end{cases} \quad (6)$$

induces a complicated harmonic measure on the boundary of the patterns in the  $z$ -plane.

## III. SCALING PROPERTIES OF THE PRODUCED FRACTAL PATTERNS

The function  $\Phi_n(w)$  in Eq. (3), has the following Laurent series expansion

$$\Phi_n(w) = F_1^{(n)}w + F_0^{(n)} + F_{-1}^{(n)}w^{-1} + \dots, \quad (7)$$

where  $F_1^{(n)}$  is called the *conformal radius* and  $F_0^{(n)}$  the *center of charge* of the cluster  $\mathcal{C}_n$ . It is possible to analytically show that [9] these coefficients contain descriptive information about the morphology of the clusters. In particular, for the coefficient of the linear term in Eq. (7), it can be shown that [9]

$$F_1^{(n)} = \prod_{k=1}^n (1 + \lambda_k)^a, \quad (8)$$

which scales with the cluster size  $n$  as

$$F_1^{(n)} \sim n^{1/d_f} \sqrt{\lambda_0}, \quad (9)$$

where  $d_f$  denotes the fractal dimension of the cluster.

Scaling behavior of the next Laurent coefficient  $F_0^{(n)}$  can also explain about the isotropicity of the clusters. For an isotropic DLA cluster, this coefficient scales according to the following relation

$$|F_0^{(n)}| \sim n^{1/d_0}, \quad (10)$$

with  $2/d_0 = 0.7$  [9]. This also holds for the anisotropic growth phenomena but with a different exponent  $d_0$ , e.g.,  $d_0 \sim 1.71$  is obtained for ADLA [10].

Since our produced patterns are anisotropic, in order to have a quantitative measure and compare them with that of the other studied models, we check the scaling relation (10), and compute the exponent  $d_0$  as a function of the opening angle  $\beta$  (for convenience, we address  $d_0$  as *anisotropy exponent*, in this paper). We compute  $F_0^{(n)}$  by using the recursion equation given in [9] for the Laurent coefficients.

#### IV. RESTRICTED HL PATTERNS WITH UNIFORM MEASURE

In this section, we investigate the effect of the restriction made on the angular distribution of the measure the mathematical plane, on the statistical properties the patterns produced by using the algorithm described in section II, with  $p(\theta_n) = \frac{1}{\beta}$  and  $0 \leq \theta_n \leq \beta$ .

We grew 400 clusters of size  $n = 10^4$ , and 30 clusters of size  $n = 10^5$  for different opening angles in the range  $4.5^\circ \leq \beta \leq 360^\circ$ . Having looked at the sample patterns shown in Fig. 1, the appearance of a wedge-like shape in the all patterns is evident. Each of the two interlimits for the distribution of  $\theta_n$ s, i.e.,  $\theta_n = 0$  and  $\beta$ , can represent itself as a boundary of the wedge (which due to the conformal maps, are not necessarily straight lines) in the physical plane. Despite that the harmonic measure in  $w$ -plane is uniform, the growth probability looks much larger around the boundaries in the  $z$ -plane. For small angles of  $\beta \lesssim 36^\circ$  there always appears only one finger with sidebranches on a boundary. For larger  $\beta$  there also exists at least one finger which has selected a boundary to grow on. In the range angle that two main branches coexist, because of the attraction of the boundaries, the average angle between branches increases by increasing  $\beta$ .

The snapshots of an example of growing cluster with  $\beta = 216^\circ$  in Fig. 2 graphically show the procedure of the branch formation in the growing fractal pattern.

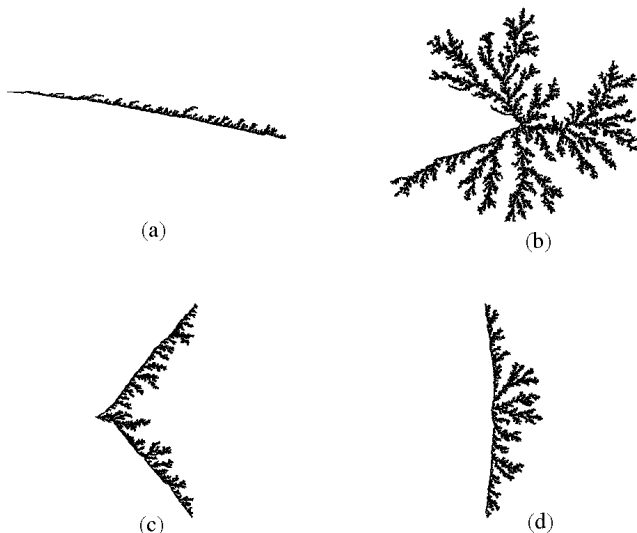


FIG. 1: Some typical clusters of size  $n = 10^5$ , generated by using the restricted HL algorithm with uniform measure and (a)  $\beta = 36^\circ$ , (b)  $\beta = 324^\circ$ , (c)  $\beta = 144^\circ$  and (d)  $\beta = 216^\circ$ .

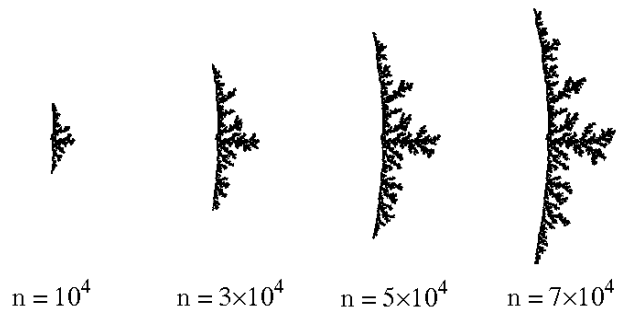


FIG. 2: Snapshots of a growing cluster of  $\beta = 216^\circ$  at different number of iterative conformal maps  $n$ .

##### A. Scaling exponents

To have a quantitative understanding of the behavior of our clusters, let us now measure some of their statistical quantities. The first quantity we would like to measure is the fractal dimension which can be obtained using the scaling relation in Eq. (9). Two sets of results, one averaged over 400 clusters of size  $10^4$  and the other over 30 clusters of size  $10^5$  at each opening angle  $\beta$ , are reported in Fig. 3. The fractal dimension shows a significant dependence on the opening angle  $\beta$ . For narrow angles the dimension takes values very close to unity which is dominated by the boundary effects. By increasing  $\beta$ , it reaches a relative maximum at around  $\beta \simeq 18^\circ$  which is almost the half-maximum angle interval in which there exists only one main branch. There also exists a local minimum of the dimension around  $\beta \simeq 144^\circ$  which seems to be a typical angle up to which only two main branches coexist. For greater angles, the dimension increases until for  $\beta = 360^\circ$  where an isotropic radial DLA with  $d_f = 1.71$  is expected. For DLA clusters in a wedge produced by the original definition [1], the fractal dimension is not affected by the wedge geometry of opening angle  $\alpha$  [20], and it depends weakly, if at all, on  $\alpha$ .

The other quantity which we measure for our clusters is the exponent describing the scaling behavior of the position of the *center of charge*  $|F_0^{(n)}|$  with the cluster size  $n$ , defined in Eq. (10). We find such a scaling behavior only in the interval  $9^\circ \leq \beta \leq 180^\circ$ . There has been also observed that the corresponding exponent  $d_0$  depends on  $\beta$  in this range. The results for two mentioned sets of averages are shown in Fig 4.

##### B. Overall shape and the morphology of the clusters

In this subsection we discuss about the overall shape and the morphology of the clusters. As mentioned before, for sectors of angle  $\beta \lesssim 36^\circ$  there exists only one main branch, and for greater angles up to  $\beta \simeq 144^\circ$  there are

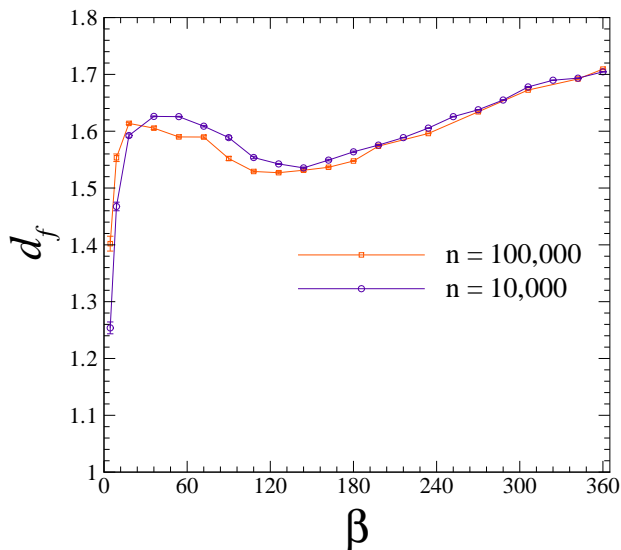


FIG. 3: The fractal dimension  $d_f$  of the patterns produced by using the restricted HL algorithm with uniform measure as a function of the opening angle  $\beta$  in  $w$ -plane. The averages were taken over 400 clusters of size  $n = 10^4$  (circles) and 30 clusters of size  $n = 10^5$  (squares).

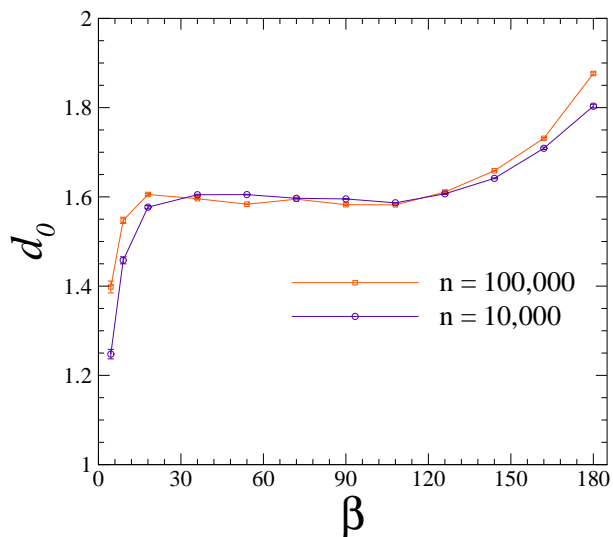


FIG. 4: The exponent  $d_0$  as a function of  $\beta$  in the scaling region, according to Eq. (10).

two main coexistent branches, and for angles  $\beta \gtrsim 144^\circ$  more than two main branches appear. To quantify this observation and obtain the average angle between two main branches of the patterns, we follow the same reasoning as in [20], for our clusters. Kessler *et al.*, [20] studied the building block of DLA clusters in a wedge by computing the angular two-point density correlation function in the constitutive sectors of a cluster.

Consider two sectors separated by angle  $\phi$ . The

density-density correlation function is then read off from

$$c(\phi) = [\langle \rho(\theta + \phi)\rho(\theta) \rangle - \langle \rho \rangle^2] / \langle \rho \rangle, \quad (11)$$

where  $\rho(\theta)$  is the density of particles in the cluster in a  $\delta\theta = 1^\circ$  sector around  $\theta$  (see Fig. 5), and  $\langle \dots \rangle$  denotes for averaging over the sectors in  $z$ -plane. The computed correlation functions for different opening angle  $\beta$  averaged over 30 realizations are shown in Fig. 6. As can be seen in the figure, for clusters consisting of one main branch there is an anticorrelation between the origin and other angles. Appearance of the second peak in the function with positive correlation is indicative of the second coexistent main branch in the cluster.

Location of the second peak shows approximately the angle between two main coexisting branches  $\eta$  in the physical plane which is reported in the second column of Table I.

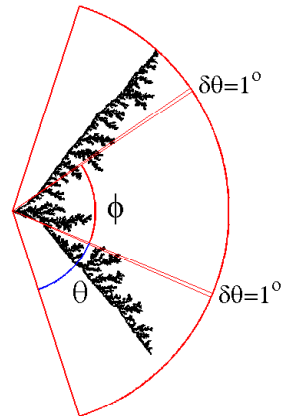


FIG. 5: Schematic description of the procedure expressed in the text to compute the angular correlation function according to Eq. (11).

For a given opening angle  $\beta$  in  $w$ -plane, the produced patterns have a wedge-like shape in the  $z$ -plane. To have an estimate relation between two angles  $\beta$  and the average opening angle of the wedge-like patterns in the  $z$ -plane  $\alpha$ , we report some of these corresponding angles in the third column of Table I. The averages are taken over 30 clusters of size  $n = 10^5$  for each reported  $\alpha$ .

$\beta$	$\eta$	$\alpha$
$36^\circ$	there is only one main branch	$15^\circ$
$90^\circ$	$31^\circ - 34^\circ$	$44^\circ$
$144^\circ$	$81^\circ - 88^\circ$	$97^\circ$
$198^\circ$	more than two main branches exist	$164^\circ$

TABLE I: The average angle between two main branches  $\eta$ , and the average opening angle of the wedge-like patterns in the  $z$ -plane  $\alpha$  for different opening angle  $\beta$  in the  $w$ -plane.

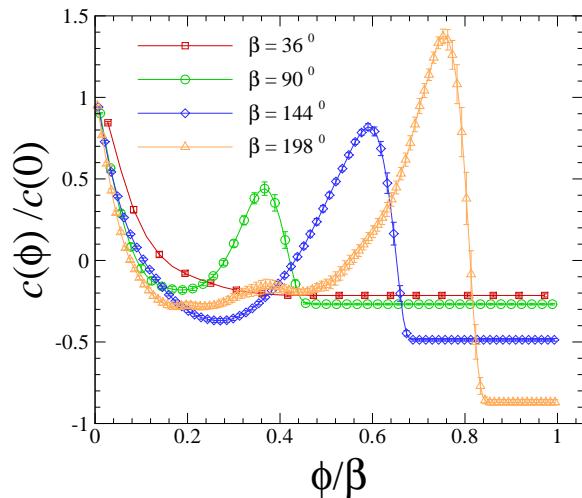


FIG. 6: Angular correlation function  $c(\phi)/c(0)$  for clusters produced by using the restricted HL algorithm with uniform measure for different opening angle  $\beta$  as a function of  $\phi/\beta$ .

## V. RESTRICTED HL PATTERNS WITH SINUSOIDAL MEASURE

As discussed in section IV, the boundary effects are evident in the visual appearance and statistical properties of the patterns. So this motivated us to force the measure to be distributed away from the boundaries i.e.,  $\theta_n = 0$  and  $\beta$  in the  $w$ -plane. By inspiration from [10], we produced patterns according to the algorithm described in section II, with  $p(\theta_n) \sim \sin(\pi\theta_n/\beta)$  for  $0 \leq \theta_n \leq \beta$ . We generated 400 clusters of size  $n = 10^4$ , and some of size  $n = 10^5$  for different opening angles in the range  $36^\circ \leq \beta \leq 360^\circ$ . Some of the clusters are shown in Fig. 7. There exists a significant difference between the overall shape of the patterns in figures 1 and 7. Due to the non-uniform measure, the visual appearance of the patterns in Fig. 7 is not affected by the boundary.

This difference can be also observed in the fractal dimension of the patterns. As plotted in Fig. 8, except for small opening angles, the fractal dimension depends weakly on  $\beta$  and takes values close to  $d_f \simeq 1.7$ .

Due to the sinusoidal distribution of the measure, even for  $\beta = 360^\circ$  the clusters are anisotropic. The growth process is dominated by advection toward a certain direction with a spatial extent which depends on the opening angle  $\beta$ . The morphology of these patterns are very similar to that of ADLA clusters.

ADLA is one of the simplest examples of transport-limited aggregation (TLA) in which the released random walkers are being drifted in the direction of a background potential flow. The difference between simulations of TLA and DLA by HL algorithm is in the sequences of the angles  $\theta_n$ . In TLA the angles are chosen from a time-dependent (non-harmonic) measure  $p(\theta, t_n)$ .

We have also examined the scaling relation Eq. (10)

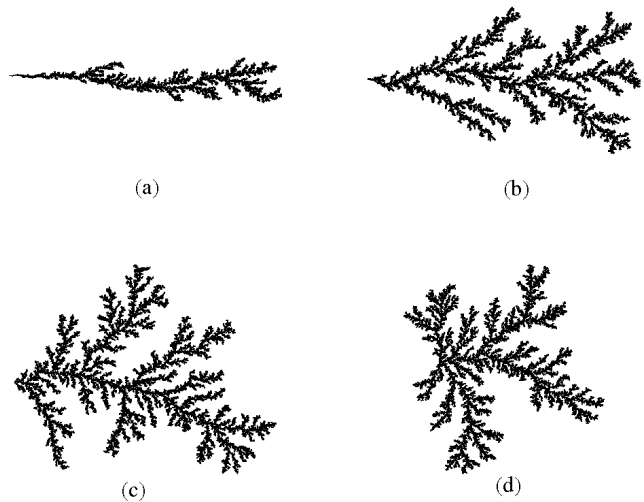


FIG. 7: Some typical clusters of size  $n = 10^5$ , generated by using the restricted HL algorithm with sinusoidal measure i.e.,  $\sin(\pi\theta_n/\beta)$  distribution and (a)  $\beta = 90^\circ$ , (b)  $\beta = 180^\circ$ , (c)  $\beta = 270^\circ$  and (d)  $\beta = 360^\circ$ .

for our clusters with sinusoidal measure and obtained the dependence of the exponent  $d_0$  on the opening angle  $\beta$ . As shown in Fig. 8,  $d_0$  is weakly dependent on  $\beta$  with values of a little less than  $d_f$  which is roughly in agreement with the same scaling behavior of ADLA which is reported in [10] for a special case  $\beta = 360^\circ$ .

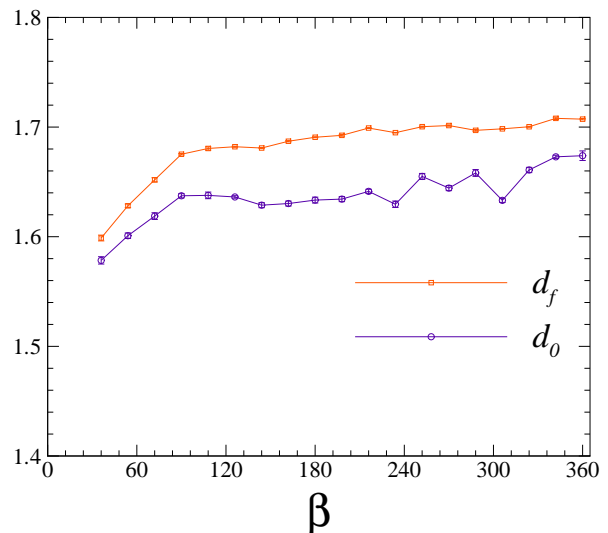


FIG. 8: The fractal dimension  $d_f$  and the scaling exponent  $d_0$  as a function of  $\beta$ , computed for the patterns generated by using the restricted HL algorithm with sinusoidal measure.

## VI. CONCLUSIONS

The fractal structure and statistical properties of the patterns generated by a generalized HL method restricted in a sector geometry were studied. It is found that the restriction with uniform measure leads to the production of fractal patterns whose fractal dimension and anisotropy exponent depend significantly to the opening angle  $\beta$  of the sector in the mathematical  $w$ -plane. The overall shape of these patterns is governed by a wedge-like DLA appearance which has been shown to be the characteristic feature of the uniform measure. The boundary effects lead to a nontrivial dependence of the average an-

gle between two major coexistence branches on the angle  $\beta$ . The proliferation of the main branches was studied by computing the angular density-density correlation function giving a quantitative understanding of the morphology of the patterns as a function of  $\beta$ .

It is also found that the sinusoidal distribution of the measure on the sectors gives fractal patterns with almost the same fractal dimension for all values  $\beta$ . The anisotropy exponent and the visual appearance of these patterns are shown to behave very similar to those of ADLA clusters.

**Acknowledgement.** A.A.S acknowledges financial support from INSF grant.

- 
- [1] T.A. Witten and L.M. Sander, *Phys. Rev. Lett.* **47**, 1400 (1981).
  - [2] L. Niemeyer, L. Pietronero, H.J. Wiesmann, *Phys. Rev. Lett.* **52**, 1033 (1984).
  - [3] R.M. Brady and R.C. Ball, *Nature (London)* **309**, 225 (1984).
  - [4] M. Matsushita, M. Sano, Y. Hayakawa, H. Honjo, Y. Sawada, *Phys. Rev. Lett.* **53**, 286 (1984).
  - [5] L. Paterson *Phys. Rev. Lett.* **52**, 1621 (1984).
  - [6] A.A. Saberi, *J. Phys.: Condens. Matter* **21**, 465106 (2009).
  - [7] M.B. Hastings and L.S. Levitov, *Physica D* **116**, 244 (1998).
  - [8] M.B. Hastings *Phys. Rev. E* **55**, 135 (1997).
  - [9] B. Davidovitch, H.G.E. Hentschel, Z. Olami, I. Procaccia, L.M. Sander, E. Somfai, *Phys. Rev. E* **59**, 1368 (1999).
  - [10] M.Z. Bazant, J. Choi, B. Davidovitch, *Phys. Rev. Lett.* **91**, 045503 (2003).
  - [11] M.G. Stepanov and L.S. Levitov, *Phys. Rev. E* **63**, 061102 (2001).
  - [12] M.N. Popescu, H.G.E. Hentschel, F. Family, *Phys. Rev. E* **69**, 061403 (2004).
  - [13] B. Davidovitch, M.J. Feigenbaum, H.G.E. Hentschel, I. Procaccia, *Phys. Rev. E* **62**, 1706 (2000).
  - [14] B.B. Mandelbrot, A. Vespignani and H. Kaufman, *Europhys. Lett.* **32**, 199 (1995).
  - [15] E. Somfai, R.C. Ball, J.P. DeVita, L.M. Sander, *Phys. Rev. E* **68**, 020401 (2003).
  - [16] M. Ben Amar, *Phys. Rev. A* **44**, 3673 (1991).
  - [17] M. Ben Amar, *Phys. Rev. A* **43**, 5724 (1991).
  - [18] A. Arneodo, J. Elezgaray, M. Tabard, F. Tallet, *Phys. Rev. E* **53**, 6200 (1996).
  - [19] L.M. Sander, E. Somfai, *Chaos* **15(2)**, 26109 (2005).
  - [20] D.A. Kessler, Z. Olami, J. Oz, I. Procaccia, E. Somfai and L.M. Sander *Phys. Rev. E* **57**, 6913 (1998).
  - [21] F. Mohammadi, A.A. Saberi, S. Rouhani, *J. Phys.: Condens. Matter* **21**, 375110 (2009).